

INVESTIGATION OF ELECTRO-MECHANICAL FACTORS EFFECTING PIEZOELECTRIC ACTUATOR FOR VALVELESS MICROPUMP CHARACTERISTICS

HAMID ASADI DERESHGI^{1,*}, MUSTAFA ZAHID YILDIZ²

¹Department of Mechatronics Engineering, Sakarya University,
54187, Sakarya, Turkey

²Department of Electrical and Electronics Engineering, Sakarya University,
54187, Sakarya, Turkey

*Corresponding Author: hamid.dereshgi@ogr.sakarya.edu.tr

Abstract

In this study, a new micropump was designed, which is suitable for medical applications regarding size and flow rate. When a micropump is used to control the amount of drug delivery, the flow rate is a key parameter and can be controlled with the diaphragm displacement. The amount of displacement depends on the thickness of the piezoelectric element, voltage, and input frequency. The simulation results showed that the displacement of the vibrating diaphragm increased with applied voltage. Moreover, when the piezoelectric thickness was increased, vibrating diaphragm displacement also was decreased. The flow rate can be adjusted by increasing or decreasing of the input voltage. Presented results also showed that the performance of the micropump was affected by the frequency of voltage. In this study, we analysed two Lead Zirconate Titanate (PZT-2) piezoelectric actuators with 50 μm and 100 μm thicknesses. The voltage values were 10 V, 20 V, 30 V, 40 V and the frequencies were 5 Hz and 10 Hz, for 3 seconds with 1 ms sensitivity. The maximum flow rate was obtained at a 50 μm thickness of PZT and its value was $3.01\text{E-}30 \text{ m}^3/\text{s}$ and the maximum displacement of the diaphragm was 1.3962 μm at 40 V and 5 Hz. Thus, the frequency and net flow rate showed an inverse correlation.

Keywords: COMSOL multiphysics, Nozzle/diffuser elements, Piezoelectric actuation.

1. Introduction

Micropumps can carry the small and precise volume of liquids for chemical, biological or medical systems [1]. Micropumps and microneedles are the essential components of the proposed drug delivery system that can actively deliver drugs in a timely manner; also, they are used for chemotherapy of cancerous patients, insulin delivery for diabetics and chronic diseases. Drug Delivery System (DDS) includes a medicine reservoir, micropumps, valves, microscopic sensors, microscopic channels and required related circuitries. Micropumps are appropriate tools for drug delivery of medicine reservoir in the body, which provides high precision and suitable for modern biotechnology drugs [2-5]. Micropumps can be used for drug delivery with the desired amount of medicines at the appropriate time, which improves the therapeutic effect. For example, in some heart diseases, the heart cannot create enough blood pressure. In this case, the micropumps are used to increase and regulate blood pressure in the pulmonary arteries [6].

Piezoelectric with silicone membrane vibrates with an electrical current in the vertical direction (indeed assuming that membrane is a silicon layer, which is an isolated fluid environment with piezoelectric). Thus, micropump chamber volume will change. When the membrane changes the location downward, the fluid inside the chamber moves out by the created pressure [7].

Choosing the material for the membrane is required for micropump performance and is determined by the purpose of the usage area. Except that the costs of the membrane should be assessed, it must be able to withstand the deformation of the biological environment. Silicon, aluminium, and copper are membrane materials that are extensively used in the literature [8].

There are various mechanisms for creating vibrations including electromagnetic, electrostatic, thermodynamic, bimetallic and shape-memory alloy [9-13]. Compared with these, the piezoelectric activity can have a good performance and provide medium pressure in less power consumption, which is preferred for medical applications [14]. Electrostatic activator needs high voltage and frequency for the displacement of the membrane in the range of a few micrometres than piezoelectric materials. Whereas, the activator acts as a memory alloy method with lower frequencies [15-16]. Hence, (another word) the benefits of the piezoelectric actuator to other irritants include fast performance, high thrusts and less power consumption [17].

Bourouina et al. [18] for the first time designed a micropump that used in the delivery of medical drugs. Maillefer et al. [19] proposed a dynamical analysis for designing drug delivery system with micropump, silicon membrane, high performance and at lower costs. Shawgo et al. [20] reviewed several plans, which are made for application of overall micro-analytical systems and delivery of drug solutions. Cui et al. [21] designed the piezoelectric micropumps showing the effects of geometric variations in the micropump, voltage, frequency, and net flow rate. Their simulation results show that at fixed frequencies, increasing the voltage increases the pump flow rate and the pressure. Also, increasing the length of the nozzle/diffuser element will increase the flow rate and reducing the diffuser angle increases the net flow rate of micropump.

There are many simulation studies in different areas for non-medical purposes. They are mainly in bigger sizes and higher flow rates. There are many studies in

the literature that is for non-medical purposes. Gerlach and Wurmus [22] and Gerlach et al. [23] for example, had a study on the output of fluid velocity (net flow rate). Their results showed that the pumping speed increases linearly with low frequency. Mu et al. [24] carried out statistical studies to optimize the piezoelectric micropump, and they used silicon, aluminium, and copper as a membrane for the piezoelectric activator. Cao et al. [25] showed that the flow rate increased at lower vibration frequency. Nguyen and Huang [26] have demonstrated that the flow rate with rising in the curvature of the activator membrane and also less vibration frequency increased. Fan et al. [27] from the University of Houston studied the impact of voltage value and frequency on the pumping speed. The simulation results indicated that pumping efficiency depends on the applied voltage to the piezoelectric because the voltage determines the amount of curvature of the membrane and the frequency, which determines the number of diaphragm vibration. They concluded that at a constant voltage, pumping performance would decrease at higher frequencies because membrane in vibration cannot reach the peak point. Wang et al. [28] studied piezoelectric activator analysis with the bronze membrane. They showed that by increasing the thickness of the membrane, the displacement would decrease significantly. Cazorla et al. [29] designed a proper micropump for liquids and gases that contain both opening and closing valves. To develop the quality of micropumps, they tested the piezoelectric in constant voltage of 24 V for lower frequencies. The maximum flow rate was achieved at 1 Hz.

The main objective of this paper is to simulate a medical purpose micropump for delivery of medicines. For this purpose, the effects of voltage, frequency and piezoelectric actuator thickness on net flow rate were simulated for the new micropump design. In section 3, the maximum flow rate results are presented and discussed.

2. Material and Methods

2.1. The mechanism of new micropump

The simulation about fabrication technologies was studied extensively with the vital parameters such as dimensions, materials, and voltages. The geometry specifications of components and materials are given in Table 1. Also, a schematic of the design is illustrated in Fig. 1. This micropump includes a pump chamber, vibrating diaphragm and two nozzle/diffuser elements that are on the left and the right sides of the chamber. The left element behaves as an input direction for the fluid from the reservoir to the pump chamber. The element in the right-side functions as an output from the pump chamber to the outside, which creates the net output flow rate. Figure 2 shows the mechanism of piezoelectric micropump with nozzle/diffuser elements. The periodic constant vibration of the diaphragm increases and decreases with the volume of the pump chamber. When piezoelectric is stimulated under the applied sinusoidal voltage, the piezo element starts to move along at the y-axis. This movement causes the fluid to be transferred from the reservoir into the micropump chamber. It is because the flow resistance in the nozzle is greater than its resistance in a diffuser. In the next half period, the diaphragm is deformed downward causing the pressure to the fluid inside the pump chamber leading from the fluent to the chamber's outlet. Thus, we will have a net flow rate for the full period.

The main goal of this paper is to obtain the maximum net flow rate. We tried to have the optimum design electromechanical parameter to increase the efficiency of the pump. According to the previous studies, because of the higher width of the chambers, the diaphragm cannot pump enough fluid throughout the chamber. Due to this adverse effect, we tried to minimize the width of the micropump chamber. The net flow rate will be higher if the chamber width is smaller and this is because the higher pressure will be applied to the fluid.

Table 1. The geometrical characteristics and intended material of micropump.

Micropumps component	Specifications
Chamber length	6000 μm
Chamber area	$6 \times 10^{-6} \text{ m}^2$
Nozzle/diffuser angle	10°
Nozzle/diffuser length	4000 μm
Membrane width	6000 μm
Membrane thickness	50 μm
Piezoelectric width	3000 μm
Piezoelectric thickness	50 μm and 100 μm
Piezoelectric material	Lead Zirconate Titanate (PZT-2)
Membrane material	Silicone
Fluid	Water

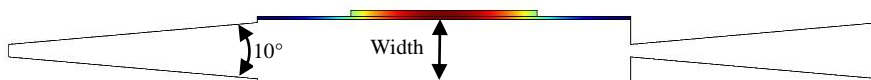


Fig. 1. A schematic of the proposed micropump.

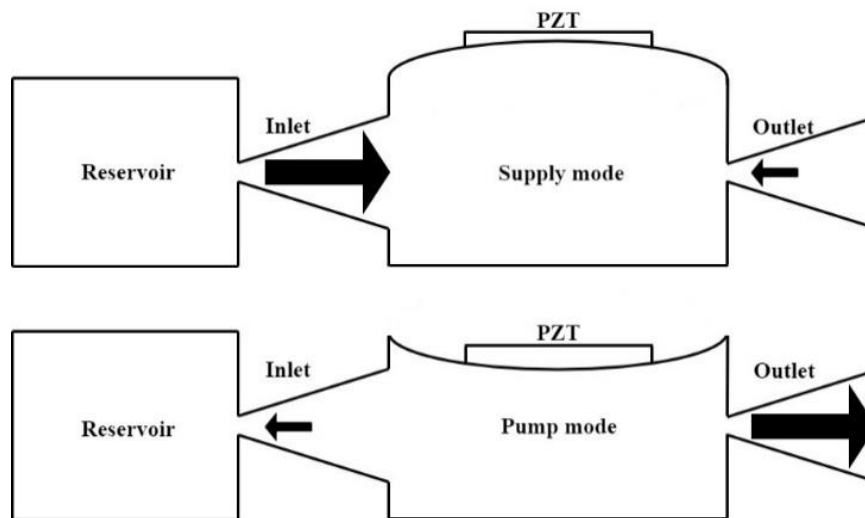


Fig. 2. The working principle of a piezo electrically-actuated valveless micropump.

2.2. Finite Element Method (FEM) analysis

Finite Element Method (FEM) is a numerical method to solve partial differential equations and also integral equations approximately. By working this way, we can ignore differential equation or simplify them to ordinary differential equations that could be solved by numerical methods like Euler. The important point in solving partial differential equations is that we can reach to a simple equation, which is numerically stable, which means that errors in the initial data may cause uncertain results. COMSOL Multiphysics software uses FEM to solve partial differential equations. This software performs finite element analysis with adaptive meshing and error control by applying different numerical solvers. The initial state of the diaphragm position is considered to examine the impact of voltage and frequency on net flow rate. The fluid motion can be calculated by the vibrational stimulus. The vibrating diaphragm and the fluid inside the chamber must be coupled together to perform this analysis. Because of the multiphysical structure of the micropump, an analytical solution is impossible. Therefore, the full Fluid-Structure Interaction (FSI) method was used for structures covering the fluid to calculate the performance characteristics of this device [30-31]. Figure 3 shows the FEM simulation of the proposed micropump design.

Infinite element method, the more elements the mesh has, the more accurate the result will be. In contrast, the calculation time will be increased. In this study, the mesh convergence study was used to obtain satisfactory diaphragm displacement results. For each PZT thickness, a separate analysis method was performed. The voltage value in the FEM analysis was 10 V and frequency was 5 Hz. In the first step, the mesh has been done with the least reasonable amount of analysis. Later, the number of mesh element was increased three more steps and repeated the analysis. The results were compared with the second, third and fourth steps with the result of the first step meshing. Having the comparison results, the mesh elements were increased further until the results saturate and no significant difference was observed. The numbers of mesh elements are shown in Tables 2 and 3. In Section 3 the results of the FEM analysis were presented and discussed.

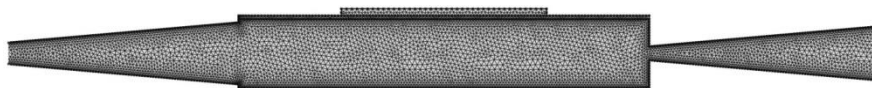


Fig. 3. FEM simulation of micropump design.

Table 2. Specifications of FEM for micropump with 50 μm PZT thickness.

Domain element statistics	Micropump with 50 μm PZT thickness			
	Coarse	Normal	Fine	Finer
Number of elements	8143	12834	21426	55993
Minimum element quality	0.1259	0.125	0.125	0.1262
Average element quality	0.8449	0.8626	0.8901	0.9078
Element area ratio	0.01154	0.006673	0.01572	0.007426
Mesh area	1.085E7 μm^2	1.085E7 μm^2	1.085E7 μm^2	1.085E7 μm^2
Maximum growth rate	3.498	3.624	3.553	3.553
Average growth rate	1.343	1.326	1.254	1.254

Table 3. Specifications of FEM for micropump with 100 μm PZT thickness.

Domain element statistics	Micropump with 100 μm PZT thickness			
	Coarse	Normal	Fine	Finer
Number of elements	7645	11887	20073	52553
Minimum element quality	0.1253	0.1251	0.1253	0.1262
Average element quality	0.8412	0.8648	0.8863	0.9071
Element area ratio	0.01037	0.006356	0.01429	0.00612
Mesh area	1.1E7 μm^2	1.1E7 μm^2	1.1E7 μm^2	1.1E7 μm^2
Maximum growth rate	3.525	3.627	3.549	3.526
Average growth rate	1.359	1.331	1.256	1.253

2.3. Fluid equations

The law of conservation of momentum and continuity equation for incompressible fluids with Newtonian viscosity has taken place in the Navier-stokes equations. Navier-stokes equation in moving mesh is written as shown in Eq. (1).

$$\rho \frac{\partial u_i}{\partial t} + \rho u_{i,j} (u_j - \hat{u}_j) = \sigma_{i,j} + \rho f_i \quad (1)$$

$$u_{i,j} = 0$$

where " u_i " shows fluid velocity, " ρ " density, " $\sigma_{i,j}$ " stress tensor, " f_i " is the body force per unit mass and " \hat{u} " is the mesh velocity [32]. Non-slip boundary conditions are thought to occur in the walls of the micropump. Controller equations show that the curvature of the membrane and the flow of liquid are always accompanied during the pumping operation.

2.4. Piezoelectric equations

MemFSI module in these matters was used in coventor ware for solving and achieving the objective. MemFSI can solve fully coupled piezoelectric problems that these challenges may be about voltage application upon piezoelectric structure deformation. Equations (2) and (3) express how the piezoelectric operates.

$$T = C^E \cdot S - e^t \cdot E \quad (2)$$

$$D = e \cdot S + \varepsilon^s \cdot E \quad (3)$$

where " T " and " S " represent the mechanical stress and strain vectors, " E " and " D " represent the electrical field and electrical displacement vector and " C^E ", " ε^s " and " e " are matrices that respectively show the matrices of hardness constant at the constant electric field, dielectric constants at constant strain and piezoelectric coupling constants [32].

2.5. Flow rectification efficiency

In nozzle/diffuser elements, the pressure loss in the input and output is more [33]. The coefficient of pressure loss across the nozzle/diffuser can be obtained from the Eq. (4).

$$K = \frac{\Delta P}{\rho_l v_l^2 l/2} \quad (4)$$

where " ΔP " is the pressure drop across the nozzle/diffuser direction, " ρ_l " is the fluid density, " v_l " the mean velocity of the fluid flow in the nozzle/diffuser elements.

The pressure is decreased throughout the nozzle/diffuser element in three parts including sudden contraction at the entrance, sudden expansion in output, gradual expansion or contraction along the length of the nozzle/diffuser element. So, the pressure coefficients " K_d ", " K_n " are decreasing across the nozzle/diffuser direction. The coefficients of pressure loss of " K_d ", " K_n " across the nozzle/ diffuser can be obtained respectively from the Eq. (5) moreover, Eq. (6).

$$K_d = K_{d,in} + K_{d,1} + K_{d,out} \left(\frac{A_1}{A_2}\right)^2 \quad (5)$$

$$K_n = K_{n,out} + (K_{n,1} + K_{n,in}) \left(\frac{A_1}{A_2}\right)^2 \quad (6)$$

" $K_{d,in}$ " is diffuser pressure loss coefficient at the inlet, " $K_{d,out}$ " diffuser pressure loss coefficient at outlet, " $K_{n,in}$ " nozzle pressure loss coefficient at inlet, " $K_{n,out}$ " nozzle of the pressure loss coefficient at outlet, " A_1 ", " A_2 " are thinnest and largest areas of nozzle/diffuser elements. Diffuser performance in the nozzle/diffuser element is defined as the ratio of pressure loss coefficient across nozzle direction with it in diffuser direction that is defined according to the Eq. (7).

$$\eta = \frac{K_n}{K_d} \quad (7)$$

If the coefficient of pressure loss in the nozzle direction is higher than it in diffuser direction, which means $\eta > 1$ pumping performance will be created from input to output. Moreover, when $\eta < 1$ pumping performance will take place from output to input.

Flow rectification efficiency in valveless micropumps can be expressed as Eq. (8).

$$\varepsilon = \frac{Q_+ - Q_-}{Q_+ + Q_-} \quad (8)$$

where " Q " represents the flow rate, and negative and positive indices are the direction of fluid flow. In other words, it indicates that the current has moving forward or backwards. Flow power efficiency represents the ability to produce micropump flow that the much more would be better [34-35].

3. Results and Discussion

The applied voltage to the piezoelectric material defines the amplitude and the frequency of vibration. The resulting flow rate will be higher if the rate of displacement of the diaphragm is bigger. Thus, the type and thickness of the piezoelectric actuator should be selected according to the applied voltage. In this study, two Lead Zirconate Titanate (PZT-2) piezoelectric actuators were analysed with the thicknesses of 50 μm and 100 μm . The voltages were from 10 V to 40 V and the frequencies were 5 Hz and 10 Hz for 3 seconds with 1ms sensitivity. In the applied FEM analysis for the central point of the diaphragm, the number of mesh elements was increased gradually. The analysis has been done for each mesh. The different types of meshes were automatically selected in the COMSOL

Multiphysics 4.3 program and each element size is presented in Tab. 2. The error rate between the first meshing step (coarse) and the second meshing step (normal) for the micropump with 50 μm and 100 μm PZT thicknesses were 10.07% and 7.08% respectively. The results of a mesh convergence analysis are given in Fig. 4.

The displacement results are given in Figs. 5 and 6. These results indicate that the diaphragm displacement increases with the increase in voltage for two frequency values. However, at constant voltages, displacements of the diaphragm in 5 Hz are more than it is at 10 Hz. So that, the maximum displacements of the diaphragm was obtained at 40 V. The displacement values at 5 Hz-10 Hz were 1.3962 μm and 0.9669 μm respectively with the PZT thickness of 50 μm . Besides that, the minimum displacements were obtained at 10 V and the values were 0.4548 μm and 0.3127 μm . In the same conditions, the maximum displacement of the diaphragm for micropump at 40 V with 100 μm PZT thickness were 0.6701 μm and 0.635 μm and minimum displacements at 10 V were 0.1511 μm and 0.1368 μm respectively.

Figures 7 and 8 show the maximum obtained flow rate from the periods of diaphragms vibration for 3 seconds. Therefore, the maximum flow rates for the micropump with 50 μm and 100 μm PZT thickness at 40 V and 5 Hz were obtained 3.01E-30m³/s and 9.30E-31m³/s respectively.

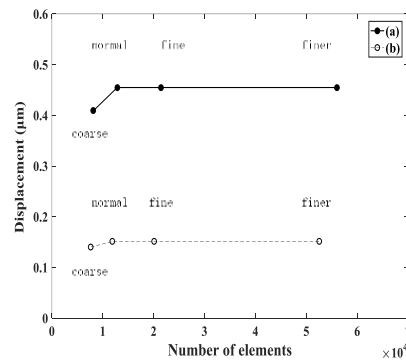


Fig. 4. Mesh convergence analysis, (a) micropump with 50 μm PZT thickness, (b) micropump with 100 μm PZT thickness.

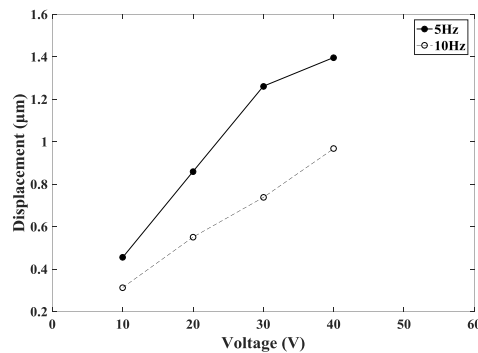


Fig. 5. Displacement of diaphragm at 5 Hz-10 Hz frequency with 50 μm PZT thickness.

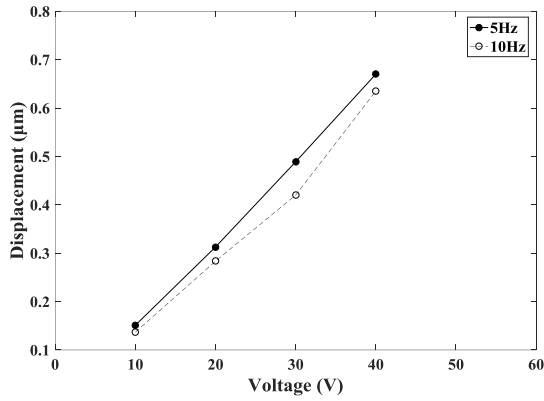


Fig. 6. Displacement of diaphragm at 5 Hz-10 Hz frequency with 100 µm PZT thickness.

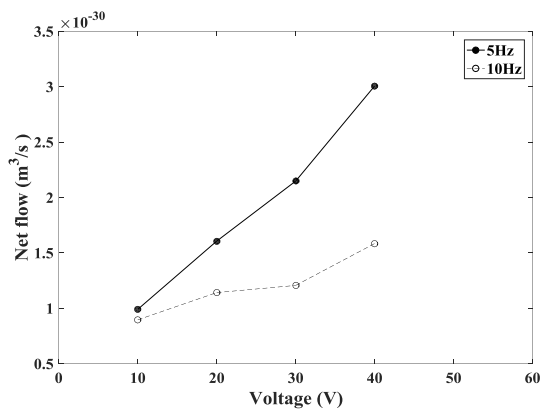


Fig. 7. A maximum flow rate of micropump at 5 Hz-10 Hz frequency with 50 µm PZT thickness.

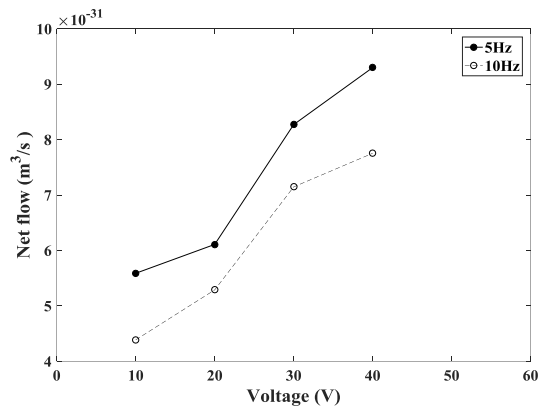


Fig. 8. A maximum flow rate of micropump at 5 Hz-10 Hz frequency with 100 µm PZT thickness.

The average resulting flow rate during this period is given in Figs. 9 and 10. Unlike other micropump structures (i.e., non-diaphragm pumps), piezoelectric actuated micropump does not create outlet flow rate in any timeframe of sinusoidal driving voltages. At the positive time course of the sinusoidal signal, suction of the fluid occurs. By contrast, at a negative portion of the signal, the micropump pumps the fluid toward the outlet. Thereby, we obtained a net outflow. The flow rate was not constant during the 3 seconds simulation period. The maximum flow rate was calculated from the COMSOL Multiphysics simulation results. Optimized parameters were tried to design in order to eliminate geometrical effects on the flow rate. For this purpose, a smaller size micropump was designed when compared to the literature to increase the efficiency. The passing net flow rate will be higher if the width of the chamber is lower. Figure 11 represents the fluid velocity vector and pressure distribution in the micropump's chamber. Piezoelectric was designed as a diaphragm actuator with two different thicknesses for voltage and frequency that analysed. Thicker piezoelectric needs higher voltages. Therefore, a piezoelectric with 50 μm thickness showed large vibration amplitude compared to piezoelectric with 100 μm thickness at the same voltage level. While choosing the piezoelectric actuator and membrane thickness, it was needed to consider corresponding micropump's chamber and to design micropump's usage area. The silicon membrane was a separator material between two states of a piezoelectric and fluid structure.

It is possible to use a micropump with 100 μm at high voltages compared to ones with 50 μm to create more pressure inside of the chamber. However, in this case, higher voltages were needed, which will not be convenient biomedical applications. The lowest recorded flow rate was measured at 10 V, and the highest value was at 40 V. Also, the stimulus frequency determines the number of diaphragm vibration, and it must be proportional to the applied voltage, piezoelectric materials, piezoelectric geometric dimensions, micropump's chamber width, and characteristics of the used fluid. The simulated fluid in this study was water.

The displacement of the diaphragm and resulting flow rate suggested that the frequency of diaphragm in 5 Hz had better performance than 10 Hz and this is because the diaphragm at the frequency of 5 Hz could reach the maximum point of vibration amplitude.

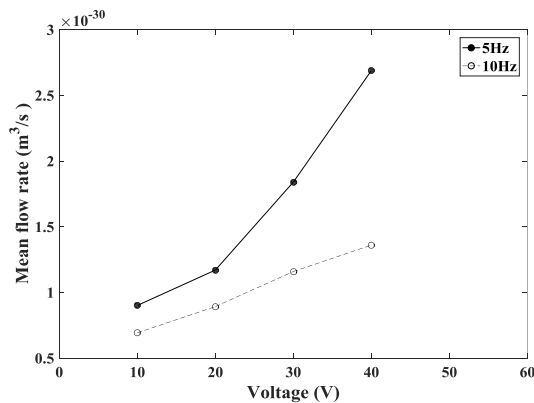


Fig. 9. The average outlet flow rate of micropump at 5 Hz-10 Hz frequency with 50 μm PZT thickness.

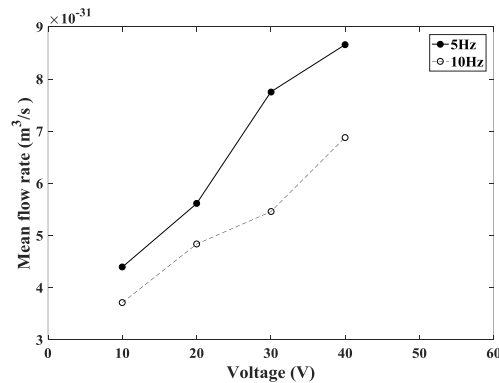


Fig. 10. The average outlet flow rate of micropump at 5 Hz-10 Hz frequency with 100 μm PZT thickness.

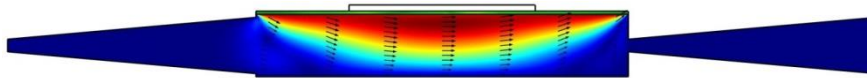


Fig. 11. Fluid velocity vector in the proposed micropump.

4. Conclusion

The obtained results show the ideal electromechanical parameters of a micropump; we examine the various parameters such as the piezoelectric thickness, effect of voltage and frequency to flow rate results. In general, it can be concluded that the piezoelectric thickness should be chosen according to the micropump dimensions and its performance. In industry, using high voltage piezoelectric may be logical, but this will not be convenient and safe for medical applications. We should design according to this situation and features. Because the clinicians may need to use an implant or invasive sensor to the patient's body to inject medicine into capillaries or directly into the patient's heart. Thereby, the applied voltage can change vibration amplitude, so we have seen that by increasing the voltage the displacements increase too. The situation was reversed for frequency. At lower frequencies, we measured a higher flow rate regardless of the voltage level. In this paper, the effects of electrical parameters were shown, which has vital importance on the net flow rate.

Acknowledgements

This study has been supported by Sakarya University Research Fund BAPK Project No: 2017-50-02-026.

Nomenclatures

A	Nozzle/diffuser areas
C^E	Matrices of hardness constant at constant electric field
D	Electrical displacement
E	Electrical field
f_l	Body force per unit mass

K	Coefficient of pressure loss across the nozzle/diffuser elements
$K_{d,in}$	Diffuser pressure loss coefficient at inlet
$K_{d,out}$	Diffuser pressure loss coefficient at outlet
$K_{n,in}$	Nozzle pressure loss coefficient at inlet
$K_{n,out}$	Nozzle pressure loss coefficient at outlet
Q	Flow rate
S	Strain vectors
T	Mechanical stress
\hat{u}	Mesh velocity
u_i	Fluid velocity
v_l	Mean velocity of the fluid flow in the nozzle/diffuser elements
Greek Symbols	
ΔP	Pressure drop across the nozzle/diffuser direction
ε	Flow rectification efficiency
ε^d	Dielectric constants
η	Ratio of the pressure loss coefficient across the nozzle direction to that in the diffuser direction
ρ	Fluid density
σ_{ij}	Stress tensor
Abbreviations	
DDS	Drug Delivery System
FEM	Finite Element Method
FSI	Fluid-Structure Interaction
PZT	Piezoelectric Zirconate Titanate

References

1. Amrani, I.; Cheriet, A.; and Feliachi, M. (2018). Design and experimental investigation of a bi-directional valveless electromagnetic micro-pump. *Sensors and Actuators A: Physical*, 272, 310-317.
2. Polla, D.L.; Erdman, A.G.; Robbins, W.P.; Markus, D.T.; Diaz-Diaz, J.; Rizq, R.; Nam, Y.; Brickner, H.T. (2000). Microdevices in medicine. *Annual Review of Biomedical Engineering*, 2, 551-576.
3. Cui, Q.; Liu, C.; and Zha, X.F.W. (2006). Design and simulation of a piezoelectrically actuated micropump for the drug delivery system. *Proceedings of the IEEE International Conference on Automation Science and Engineering*. Shanghai, China, 45-50.
4. Smits, J.G. (1990). Piezoelectric micropump with three valves working peristaltically. *Sensors and Actuators A: Physical*, 21(1-3), 203-206.
5. McAllister, D.V.; Allen, M.G.; and Prausnitz, M.R. (2000). Microfabricated microneedles for gene and drug delivery. *Annual Review of Biomedical Engineering*, 2, 289-313.
6. Zordan, E.; Amirouche, F.; and Zhou, Y. (2010). Principle design and actuation of a dual chamber electromagnetic micropump with coaxial cantilever valves. *Biomedical Microdevices*, 12(1), 55-62.

7. He, X.; Zhu, J.; Zhang, X.; Xu, L.; and Yang, S. (2017). The analysis of internal transient flow and the performance of valveless piezoelectric micropumps with planar diffuser/nozzles elements. *Microsystem Technologies*, 23(1), 23-37.
8. Ashraf, M.W.; Tayyaba, S.; and Afzulpurkar, N. (2011). Micro electromechanical systems (MEMS) based microfluidic devices for biomedical applications. *International Journal of Molecular Sciences*, 12(6), 3648-3704.
9. Hatch, A.; Kamholz, A.E.; Holman, G.; Yager, P.; and Bohringer, K.F. (2001). A ferrofluidic magnetic micropump. *Journal of Microelectromechanical Systems*, 10(2), 215-221.
10. Zengerle, R.; Ulrich, J.; Kluge, S.; Richter, M.; and Richter, A. (1995). A bidirectional silicon micropump. *Sensors and Actuators A: Physical*, 50(1-2), 81-86.
11. Jeong, O.C.; and Yang, S.S. (2000). Fabrication and test of a thermopneumatic micropump with a corrugated p+ diaphragm. *Sensors and Actuators A: Physical*, 83(1-3), 249-255.
12. van Lintel, H.T.G.; van De Pol, F.C.M.; and Bouwstra, S. (1988). A piezoelectric micropump based on micromachining of silicon. *Sensors and Actuators*, 15(2), 153-167.
13. Joshitha, C.; Sreeja, B.S.; and Radha, S. (2017). A review on micropumps for drug delivery system. *Proceedings of the IEEE International Conference Wireless Communications, Signal Processing and Networking (WiSPNET)*. Chennai, India, 186-190.
14. Sateesh, J.; Sravani, K.G.; Kumar, R.A.; Guha, K.; and Rao, K.S. (2018). Design and flow analysis of MEMS based piezo-electric micro pump. *Microsystem Technologies*, 24(3), 1609-1614.
15. Yufeng, S.; Wenyan, C.; Feng, C.; and Weiping, Z. (2006). Electromagnetically actuated valveless micropump with two flexible diaphragms. *The International Journal of Advanced Manufacturing Technology*, 30(3-4), 215-220.
16. Yu-feng, S.; Wen-yuan, C; Feng, C.; and Wei-ping, Z. (2007). Design and fabrication process of electromagnetically actuated valveless micropump with two parallel flexible diaphragms. *Journal of Shanghai University (English Edition)*, 11(1), 79-83.
17. He, X.; Xu, W.; Lin, N.; Uzoejinwa, B.B.; and Deng, Z. (2017). Dynamics modeling and vibration analysis of a piezoelectric diaphragm applied in valveless micropump. *Journal of Sound and Vibration*, 405, 133-143.
18. Bourouina, T.; Bossebuf, A.; and Grandchamp, J.-P. (1997). Design and simulation of an electrostatic micropump for drug-delivery applications. *Journal of Micromechanics and Microengineering*, 7(3), 186-188.
19. Maillefer, D.; Gamper, S.; Frehner, B.; Balmer, P.; van Lintel, H.; and Renaud, P. (2001). A high-performance silicon micropump for disposable drug delivery systems. *Proceedings of the 14th IEEE International Conference on Micro Electro Mechanical Systems*. Interlaken, Switzerland, 413-417.
20. Shawgo, R.S.; Grayson, A.C.R.; Li, Y.; and Cima, M.J. (2002). BioMEMS for drug delivery. *Current Opinion in Solid State and Materials Science*, 6(4), 329-334.

21. Cui, Q.; Liu, C.; and Zha, X.F. (2008). Simulation and optimization of a piezoelectric micropump for medical applications. *The International Journal of Advanced Manufacturing Technology*, 36(5-6), 516-524.
22. Gerlach, T.; and Wurmus, H. (1995). Working principle and performance of the dynamic micropump. *Sensors and Actuators A: Physical*, 50(1-2), 135-140.
23. Gerlach, T.; Schuenemann, M.; and Wurmus, H. (1995). A new micropump principle of the reciprocating type using pyramidal micro flowchannels as passive valves. *Journal of Micromechanics and Microengineering*, 5(2), 199-201.
24. Mu, Y.H.; Hung, N.P.; and Ngoi, K.A. (1999). Optimisation design of a piezoelectric micropump. *The International Journal of Advanced Manufacturing Technology*, 15(8), 573-576.
25. Cao, L.; Mantell, S.; and Polla, D. (2001). Design and simulation of an implantable medical drug delivery system using microelectromechanical systems technology. *Sensors and Actuators A: Physical*, 94(1-2), 117-125.
26. Nguyen, N.T.; and Huang, X. (2001). Miniature valveless pumps based on printed circuit board technique. *Sensors and Actuators A: Physical*, 88(2), 104-111.
27. Fan, B.; Song, G.B.; and Hussain, F. (2005). Simulation of a piezoelectrically actuated valveless micropump. *Smart materials and structures*, 14(2), 400-405.
28. Wang, B.; Chu, X.; Li, E.; and Li, L. (2006). Simulations and analysis of a piezoelectric micropump. *Ultrasonics*, 44(22), e643-e646.
29. Cazorla, P.-H.; Fuchs, O.; Cochet, M.; Maubert, S.; Le Run, G.; Fouillet, Y.; and Defay, E. (2016). A low voltage silicon micro-pump based on piezoelectric thin films. *Sensors and Actuators A: Physical*, 250, 35-39.
30. Pan, L.S.; Ng, T.Y.; Liu, G.R.; Lam, K.Y.; and Jiang, T.Y. (2001). Analytical solutions for the dynamic analysis of a valveless micropump—a fluid-membrane coupling study. *Sensors and Actuators A: Physical*, 93(2), 173-181.
31. Zhou, Y.; and Amirouche, F. (2009). Study of fluid damping effects on resonant frequency of an electromagnetically actuated valveless micropump. *The International Journal of Advanced Manufacturing Technology*, 45(11), 1187-1196.
32. Johari, J.; and Majlis, B.Y. (2008). Flow behaviour of fluid-structure interaction (FSI) system of piezoelectric actuated valveless micropump (PAVM). *Proceedings of the IEEE International Conference on Semiconductor Electronics. Johor Bahru, Malaysia*, 216-220.
33. Lee, C.-J.; Sheen, H.-J.; Tu, Z.-K.; Lei, U.; and Yang, C.-Y. (2009). A study of PZT valveless micropump with asymmetric obstacles. *Microsystem Technologies*, 15(7), 993-1000.
34. Singhal, V.; Garimella, S.V.; and Murthy, J.Y. (2004). Low Reynolds number flow through nozzle-diffuser elements in valveless micropumps. *Sensors and Actuators A: Physical*, 113(2), 226-235.
35. Wang, Y.-C.; Hsu, J.-C.; Kuo, P.-C.; and Lee, Y.-C. (2009). Loss characteristics and flow rectification property of diffuser valves for micropump applications. *International Journal of Heat and Mass Transfer*, 52(1-2), 328-336.